http://www.jstage.jst.go.jp/browse/biophysics

BIOPHYSICS

REVIEW

Vol. 8, pp. 59–66 (2012)
doi: 10.2142/biophysics.8.59

Coordinated regulation of multiple flagellar motors by the *Escherichia coli* chemotaxis system

Hajime Fukuoka[1], Yuichi Inoue[1] and Akihiko Ishijima[1]

[1]*Institute of Multidisciplinary Research for Advanced Materials, Tohoku University, Aoba-ku, Sendai 980-8577, Japan*

Received October 5, 2011; accepted January 29, 2012

Escherichia coli **cells swim toward a favorable environment by chemotaxis. The chemotaxis system regulates the swimming behavior of the bacteria by controlling the rotational direction of their flagellar motors. Extracellular stimuli sensed by chemoreceptors are transduced to an intracellular signal molecule, phosphorylated CheY (CheY-P), that switches the rotational direction of the flagellar motors from counterclockwise (CCW) to clockwise (CW) or from CW to CCW. Many studies have focused on identifying the proteins involved in the chemotaxis system, and findings on the structures and intracellular localizations of these proteins have largely elucidated the molecular pathway. On the other hand, quantitative evaluations of the chemotaxis system, including the process of intracellular signaling by the propagation of CheY-P and the rotational switching of flagellar motor by binding of CheY-P molecules, are still uncertain. For instance, scientific consensus has held that the flagellar motors of an *E. coli* cell switch rotational direction asynchronously. However, recent work shows that the rotational switching of any two different motors on a single *E. coli* cell is highly coordinated; a sub-second switching delay between motors is clearly correlated with the relative distance of each motor from the chemoreceptor patch located at one pole of the cell. In this review of previous studies and our recent findings, we discuss the regulatory mechanism of the multiple flagellar motors on an individual *E. coli* cell and the intracellular signaling process that can be inferred from this coordinated switching.**

Corresponding author: Hajime Fukuoka, IMRAM, Tohoku University, Aoba-ku, Sendai 980-8577, Japan.
e-mail: f-hajime@tagen.tohoku.ac.jp

Key words: signal transduction, rotary motor, bacteria, CheY, receptor

Signal transduction systems are widely conserved in a wide range of living organisms[1–4], and are essential for cells to respond to chemical and mechanical changes. Many bacteria, including the peritrichously flagellated *Escherichia coli*, can seek out environments conducive to their growth. In a phenomenon called chemotaxis, the *E. coli* cell swims toward attractant chemicals, such as serine and aspartate, and away from repellent chemicals, such as Ni^+ and indole, by rotating its flagella (Fig. 1a). Each flagellum is powered by a bidirectional rotary motor embedded in the cell membrane. When all of the flagellar motors are rotating counterclockwise (CCW), the left-handed normal helical flagellar filaments form a bundle, and the *E. coli* cell swims smoothly. When one or more of the motors switches to a clockwise (CW) rotation, the bundle is disrupted and the cell tumbles. The cell orients in a new direction when the normal to semi-coiled polymorphic transformation of flagellar filaments is complete. The cell attains its initial swimming speed when the motors switch back to CCW and the filaments rejoin the bundle[5]. When the cell swims toward a high concentration of attractant chemicals, it swims smoothly by continuous CCW rotation of the motor. When the cell swims toward lower attractant concentrations, it switches the rotational direction of the motor and tumbles more frequently. Therefore, the cell's chemotactic migration toward favorable conditions is determined by the duration of smooth swimming and tumbling frequency (Fig. 1a, 1b).

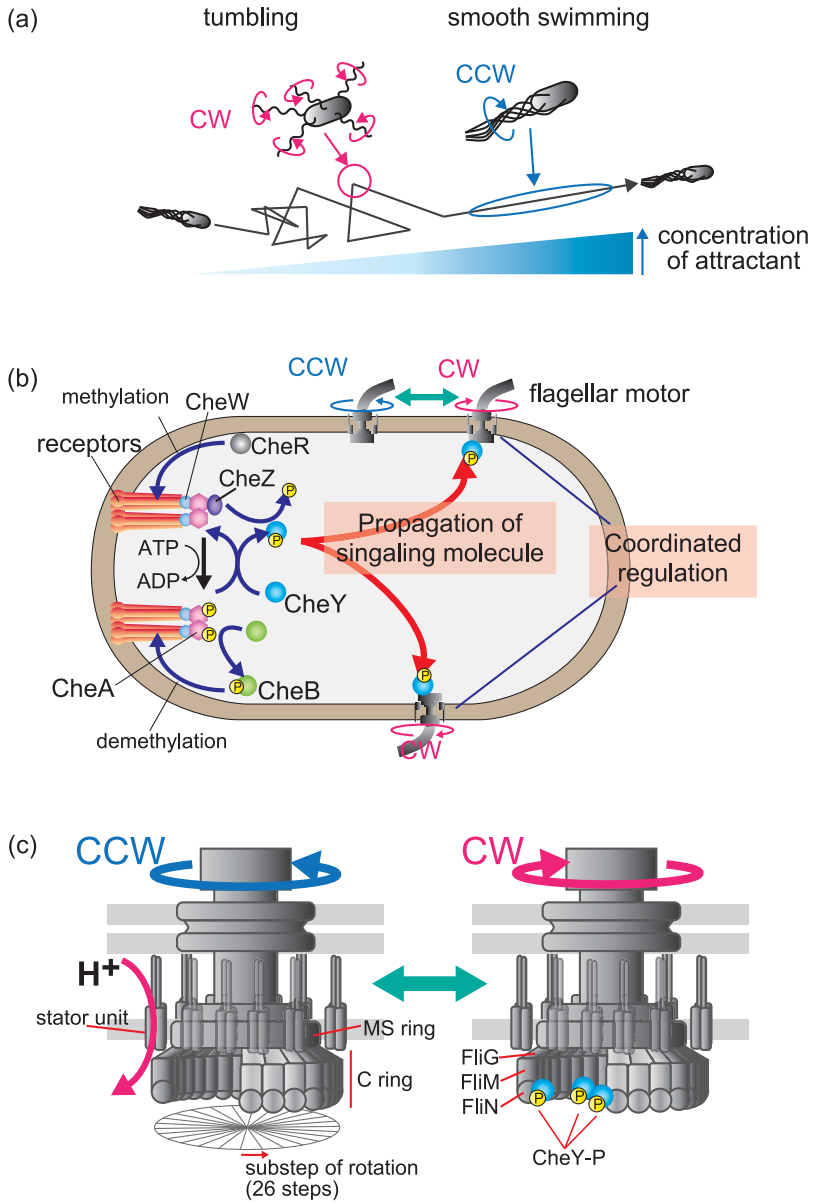

Figure 1 The chemotaxis system in *E. coli*. (a) *E. coli* chemotactic response. Cells in a liquid environment alternate between smooth swimming and tumbling, which are regulated by the rotational direction of flagellar motors. Cells swim smoothly when all the motors rotate counterclockwise (CCW) and flagellar filaments form a bundle. Cells tumble when the motors switch to clockwise (CW) rotation and the bundle is disrupted. *E. coli* cells swim against the gradient of the concentration of an attractant by regulating their smooth swimming and tumbling via the chemotaxis system. (b) The chemotaxis molecular pathway. Chemotactic signals, such as chemicals, pH, and temperature, are detected by chemoreceptors located primarily at one of the cellular poles. Thousands of receptor proteins cluster in patches with CheA and CheW. Receptors increase CheA autophosphorylation when they sense a repellent or a decrease in attractant. The phosphoryl group on CheA is transferred to a response regulator, CheY. Phosphorylated CheY (CheY-P) binds to the flagellar motor and increases the probability of its CW rotation. The binding of attractant chemicals to receptors inhibits CheA autophosphorylation. In addition to this inhibition, CheZ reduces the intracellular concentration of CheY-P. As a result, the motor continues to rotate CCW. CheR and CheB regulate chemotaxis via the methylation and demethylation of receptors, respectively. Decreased attractant levels (or a sensing of repellent) induce the phosphorylation of CheB to demethylate receptors, which decreases CheA autophosphorylation. The binding of attractants to receptors reduces the phosphorylation and activity of CheB, and the receptors are methylated by CheR; this methylation increases CheA autophosphorylation. This negative feedback is called adaptation. (c) *E. coli* flagellar motor structure and properties. The motor consists of a rotor and several stator units, which act as torque generators that convert H^+ flux energy into motor rotation. Several kinds of proteins assemble to form ring structures within the rotor: approximately 26 copies of FliG, 34 copies of FliM, and over 100 copies of FliN assemble to form the C-ring. The motor rotates, repeating 26 angular steps per revolution. In the absence of CheY-P, the motor rotates CCW. The binding of CheY-P to FliM (and FliN) increases the probability of CW rotation.

Bacterial flagellar motor

The bacterial flagellar rotary motor is driven by the flux of coupling ions across the cell membrane (Fig. 1c). The coupling ion differs according to the type of motor and/or bacterial species. *E. coli* and *Salmonella enterica* motors use the H^+ [6,7], and those of the alkaliphilic *Bacillus* and marine *Vibrio* species utilize Na^+ [8,9]. *Shewanella oneidensis* MR-1 has distinct stators that couple to Na^+ or H^+ flux; both types of stators are thought to function in the same motor[10]. The stator in the alkaliphilic *Bacillus clausii* utilizes Na^+ at high pH, but H^+ at low pH[11]. The H^+-driven motor of *E. coli* rotates at about 350 Hz (zero-torque speed) and generates a maximum torque of about 1300 pN nm[12,13]. Both the H^+-driven motor of *Salmonella* and a Na^+-driven chimeric motor reconstituted in *E. coli* rotate by repeating 26 angular steps per revolution, which is consistent with the periodicity of the FliG subunits in the motor structure[14,15] (Fig. 1c).

The motor of *E. coli* consists of a rotor and at least 11 stator units surrounding the rotor structure[6,16] (Fig. 1c). The stator unit is thought to be a torque generator that converts ion flux energy into mechanical work. The rotor part is believed to consist of two main structures, known as the MS-ring and the C-ring. Multiple FliF proteins assemble to form the MS-ring in the cytoplasmic membrane, and 34 copies of FliM and more than 100 copies of FliN assemble to form the main structure of the C-ring. It is thought that 26 copies of FliG attach to the MS-ring and connect the C-ring to the flagellar structure. The recent work shows that stator units are exchanged frequently in functioning motors in H^+-driven motor of *E. coli*[17]. In the Na^+-driven motor of *Vibrio*, the coupling ion regulates the assembly and disassembly of stator units into the motor[18]. Furthermore, the rotor component proteins FliM and FliN are exchanged in functioning motors[19,20].

The *E. coli* chemotaxis system

The chemotaxis system regulates the swimming behavior of cells by controlling the rotational direction of flagellar motors in response to extracellular stimuli, such as chemicals, pH, and temperature. Studies using biochemical, biophysical, genetic, and structural approaches have identified many of the proteins involved in chemotaxis, and a hypothesis of the molecular pathway of the chemotaxis system has been proposed (Fig. 1b). Extracellular chemicals are detected by transmembrane chemoreceptors localized primarily at one of the cellular poles, where thousands of chemoreceptor proteins cluster in patches[21,22]. The chemoreceptors appear to be organized into units of trimers of dimers in the patches[23]. Each chemoreceptor has a periplasmic ligand-binding domain and a cytoplasmic signaling domain[4,24,25] and forms a ternary complex with the cytoplasmic histidine protein kinase, CheA, and an adaptor protein, CheW[21,26–28]. In this complex, CheW links CheA to the signaling domain of the chemoreceptor. A recent report showed that the core structural and functional unit consists of two receptor trimers of dimers, two CheW molecules, and a CheA dimer[29].

When the ligand-binding domain of a receptor senses a chemotactic signal, it modulates the autophosphorylation activity of CheA. The chemoreceptor increases the autophosphorylation of CheA in response to a repellent or to a reduced concentration of attractant (Fig. 1b)[30,31]. The phosphoryl group of CheA is rapidly transferred to a response regulator, CheY. Phosphorylated CheY (CheY-P), an intracellular signaling molecule, is released from the chemoreceptor patch. The binding of CheY-P to the FliM subunit of the flagellar motor induces the switching of the motor's rotational direction from CCW to CW[32], which increases the tumbling frequency of the cell. In a recent model, CheY-P interacts with FliN after being first captured by FliM, and this process promotes the rotational switching of the motor[33]. The CW-motor bias (fraction of time spent in CW rotation) is known to be highly cooperative to the intracellular concentration of CheY-P, and it change drastically above a certain concentration of CheY-P[34]. The CheY-P-induced switch in the motor rotation appears to be stochastic rather than deterministic: CheY-P binding determines only the probability of CW or CCW rotation in stochastic model[35]. The intracellular signal is terminated by the dephosphorylation of CheY-P by CheZ, which is mainly localized to the chemoreceptor patch via the short form of CheA[36]. In contrast, when a chemoreceptor binds to an attractant chemical, it inhibits CheA autophosphorylation. Subsequently, CheZ reduces the intracellular concentration of CheY-P (Fig. 1b). As a result, the cell swims smoothly due to the continuous CCW rotation of its motors.

E. coli cells reset their chemotaxis system to adapt to changes in the concentration of chemical stimuli over a wide dynamic range. This adaptation is regulated by CheR and CheB, which methylates and demethylates chemoreceptors, respectively (Fig. 1b). In adaptation, the phosphoryl group of CheA is transferred to CheB in response to a repellant or a reduced concentration of attractant. Phosphorylated CheB demethylates chemoreceptors to reduce the autophosphorylation of CheA. However, the binding of an attractant reduces the phosphorylation and activity of CheB, allowing the receptors to be methylated by the constitutively active methyltransferase CheR. The methylated chemoreceptors increase the autophosphoryaltion activity of CheA.

The model of chemotaxis molecular pathway described above was constructed from studies on the roles and localization of proteins involved in the system. However, quantitative evaluations in signaling process, such as intracellular signaling, directional switching of a single flagellar motor, and the coordination of multiple flagellar motors on a single cell, are still uncertain. These parameters should be examined quantitatively to clarify the mechanism of the chemotaxis system.

Previous rotational measurements of multiple flagellar motors on a single bacterial cell

Each *E. coli* cell has multiple flagella—8.5 on average, in liquid medium[37]—that must be coordinately regulated in response to extracellular chemotactic signals. In 1983, the rotation of multiple flagellar motors was directly measured to clarify the regulatory mechanism of multiple motors. Macnab and Han measured the rotational directions of multiple motors in *Salmonella* by observing the shape of the flagellar filament, which changes with the rotational direction of the motor[38]. They observed the asynchronous motions of two flagella driven by mutant motors to have a strong CW bias, when viewed at 1-s intervals. Ishihara and colleagues simultaneously measured the rotational directions of multiple motors on artificial filamentous cells via the rotation of a small marker cell (about 10 Hz) attached to each motor[39]. They reported that the rotational switching of motors occurs asynchronously; however, the variations in CCW bias (the fraction of time spent in CCW rotation) were correlated among the motors. These results were interpreted to mean that transitions between the CCW and CW states occur at random times, but the rates at which these transitions occur are subject to coordinated control.

Coordinated regulation between two flagellar motors in a single *E. coli* cell

The idea and the techniques of previous works were innovative both conceptually and technically, however, we considered the possibility that these previous experiments might have been affected by some artificial modifications. Recent advances in experimental techniques enabled us to detect, for the first time, a high correlation in directional switching between motors[40]. We measured the rotation of motor in the *E. coli* cell under more native condition; well-energized motors (rotating at about 150 Hz) on normal-sized cells (< 3 μm long) were subjected to a tethered-bead assay using a high-speed camera (Fig. 2a)[15,20,40,41]. The high spatial (1 nm) and temporal (0.8 ms) resolutions were confirmed in our measurement system. Our results clearly showed that the directional switching between two motors is highly coordinated (Fig. 2b). A correlation analysis was performed on the time traces of the rotational directions between two motors, and the switching coordination was represented as a major peak with a time delay of nearly 0 s in the correlation profile (Fig. 2c) (see the methods in reference 40). We also showed that coordinated switching is dictated by the intracellular signaling molecule CheY-P, since switching was not coordinated in a deletion mutant of the *cheZ* gene (CheZ dephosphorylates CheY-P), or in cells expressing a constitutively active CheY mutant protein that mimics the CW-rotation-stimulating function of CheY-P[42]. These results indicate that a transient increase or decrease in the intracellular CheY-P concentration directly triggers coordinated

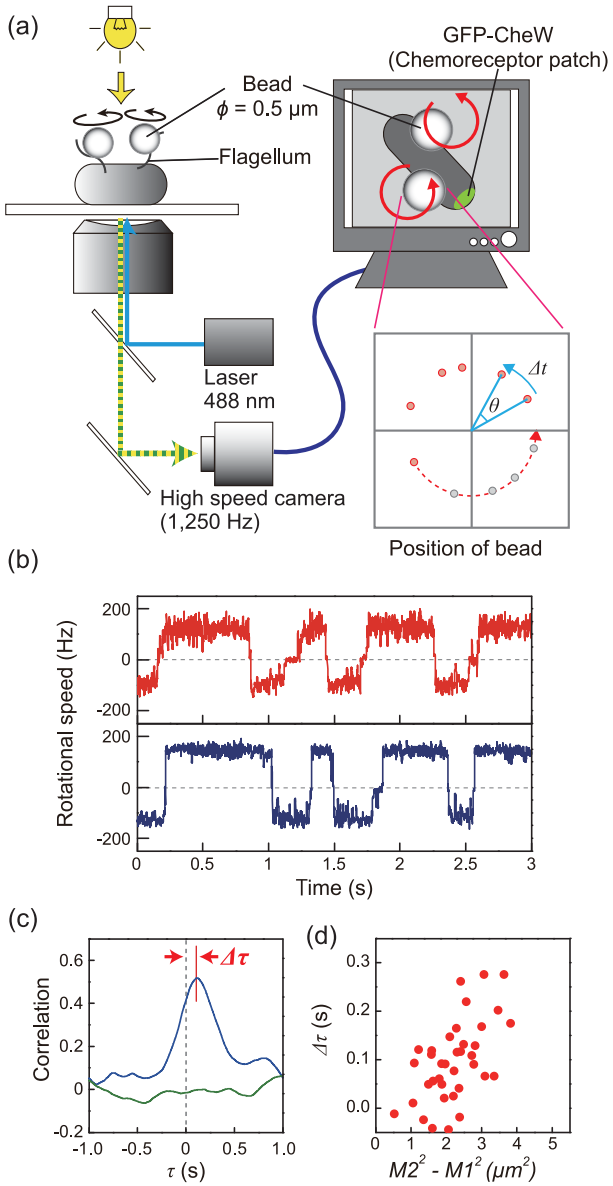

Figure 2 Coordinated switching of multiple flagellar motors in a single *E. coli* cell. (a) Schematic diagram of the measurement system. Polystyrene beads (ϕ=0.5 μm) were attached to sticky flagellar stubs. Phase-contrast images of each bead were recorded with a high-speed CCD camera, and the angular velocity and rotational direction were estimated from the position of the bead for every recorded frame. The chemoreceptor patch was observed via the intracellular localization of GFP-CheW. (b) Time course of the rotational speeds of two motors on the same cell. Plus and minus values represent CCW and CW rotations, respectively. Lines indicate the speed of the motor closer to (red) and farther from (blue) the chemoreceptor patch. The motor closer to the patch switched rotational direction before the more distant motor, in both CCW-to-CW and CW-to-CCW switching. (c) Correlation analysis of the switching between the two motors depicted in Fig. 2b (blue line). The green line shows the correlation between two motors on a different cell. Delay of the peak was defined as Δτ, which represents the difference in the time of switching between two motors. (d) The relationship between Δτ and $M2^2$–$M1^2$, where *M1* and *M2* are the distances from the chemoreceptor patch to the closer and further motors, respectively. Correlations were analyzed based on the motor closer to the major chemoreceptor patch. Part b, c, and d of the figure was reused with permission from reference 40.

switching between motors. Our study provided new insights for reconstructing the model of the chemotaxis system.

Propagation of the intracellular signal in an *E. coli* cell

CheY-P molecules probably diffuse through the cytoplasm, although this has not been directly measured. We inferred the intracellular signaling process from the switching delay between two motors and their relative distance from the chemoreceptor patch (the patch location was observed via GFP-fused CheW) (Fig. 2a)[40]. The results showed that in both CCW-to-CW and CW-to-CCW switching, a motor closer to the chemoreceptor patch switches earlier than a more distant one (Fig. 2b). The difference in the time of switching between motors was represented as the delay time of the peak of correlation ($\Delta\tau$), and the $\Delta\tau$ values clearly correlated with the relative distance of each motor from the chemoreceptor patch (Fig. 2c, 2d). From these results, we proposed that CheY-P molecules are typically produced intermittently and diffuse from the chemoreceptor patch, and that each transient change in CheY-P concentration is propagated to each motor with a delay time correlated with its distance from the chemoreceptor patch.

An intracellular signaling model

Previous studies indicated that motors on the same *E. coli* cell switch rotational direction asynchronously[38,39], while variations in bias are correlated between motors[39]. Therefore, in *E. coli* cell, the switching of rotational direction of motor has been interpreted to occur stochastically, while the bias of motor rotation are coordinately controlled. In contrast to previous study, we showed that motors on the same cell coordinately switch rotational direction[40]. To explain the coordinated switching of multiple flagellar motors, the timing of CCW-to-CW and CW-to-CCW switching should be determined by an increase and decrease in CheY-P concentration, respectively. Thus, a change in CheY-P concentration should occur for every switching event (Fig. 3).

We also reported that a subsecond delay in the coordinated switching between motors that correlates with the distance of each motor from the chemoreceptor patch (Fig. 2d), and that the switching of a motor closer to the receptor patch precedes that of a motor farther from the patch in both CCW-to-CW and CW-to-CCW switching (Fig. 2b). To explain the coordinated switching with a delay between motors, the dynamic changes in CheY-P concentration, such as a sudden increase or decrease, should occur at motors closer to the chemoreceptor patch first, and the concentration change then follows similarly at motors farther from the patch (Fig. 3). Therefore, we proposed that wave-like changes in CheY-P concentration are propagated from the receptor patch to each motor and constitute the intracellular signal. Cluzel *et al.*[34] reported that the CW bias of a motor is

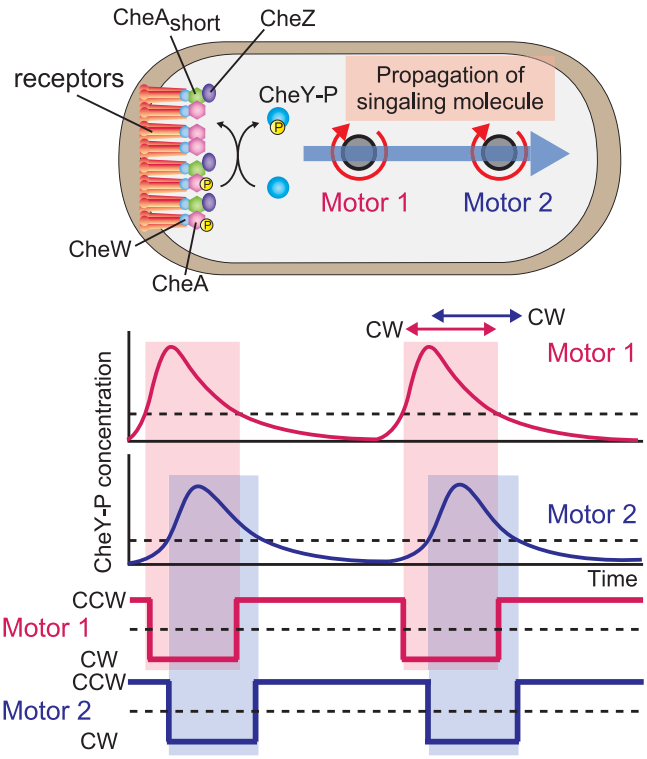

Figure 3 An intracellular signaling model. CheY-P is produced intermittently at the chemoreceptor patch, and the increases or decreases in CheY-P concentration are propagated like a wave, reaching motors at different positions on the cell with a delay time (top and middle) and triggering coordinated switching between them (bottom). When the CheY-P concentration change is above and below a threshold (broken lines depicted in middle panels), the motor switches from CCW to CW and CW to CCW, respectively. The signal is terminated by CheZ, which associates with the chemoreceptor patch via the short form of CheA, indicating that the signal is generated and terminated at the receptor patch.

highly cooperative to the intracellular concentration of CheY-P. Therefore, the transient change in CheY-P concentration that alters the CW bias from 0 to 1 should occur with every switching event to coordinate the switching of multiple flagellar motors.

The regulation of flagella in a swimming cell

The relationship between swimming behavior and the formation of the flagellar bundle has been discussed in previous works[43,44]. When all the flagellar motors are rotating CCW, the flagellar filaments form a bundle, and the *E. coli* cell swims smoothly. On the other hand, the flagellar bundle is disrupted when the motors switch to the CW rotation, and the cell tumbles. By observing fluorescently labeled flagellar filaments in a swimming cell, Turner *et al.*[43] showed that the angular change in swimming direction increases with the number of CW-rotating filaments that escape from the flagellar bundle. This suggested that the switching of the flagellar motor is coordinated in a swimming cell as well as

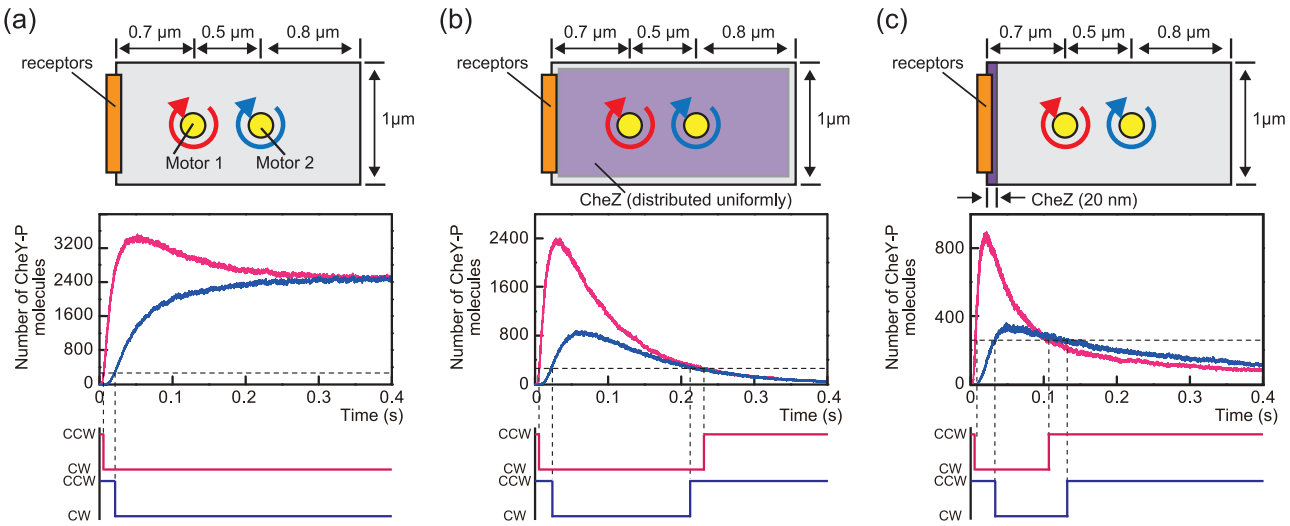

Figure 4 A simulation of the relationship between CheY-P propagation and CheZ intracellular localization. In this simulation, a rectangle with 2-μm long and 1-μm wide was assumed the cell; 25,000 CheY-P molecules were generated at the left side edge of the rectangle (shown as receptors in the illustrations in the top panels) and diffused in two dimensions with a diffusion coefficient of 5 $\mu m^2/s$. The motors were positioned 0.7 (motor 1) and 1.2 μm (motor 2) from the receptor patch, and the number of CheY-P molecules around the position of each motor was counted. Graphs shown in the middle panels indicate the time courses for the number of CheY-P molecules that was counted near motor 1 (red lines) and motor 2 (blue lines). The horizontal broken lines in the graphs indicate the arbitrary threshold of CheY-P molecules set to trigger the rotational direction switching of the motors (260 counts was assumed as the threshold). The bottom panels show the time course of the rotational direction of motors inferred from the corresponding changes in CheY-P counts shown in the middle panels. (a) Simulations in the absence of CheZ (averaged trace of 3 independent calculations). (b) Simulations in which CheZ was assumed to be uniformly distributed in the rectangle (averaged trace of 3 independent calculations). The probability of dephosphorylation was set to 0.0004 in the cytoplasm (2 μm in length and 1 μm in width). (c) Simulations in which CheZ was assumed to be localized within 20 nm of one rectangle edge (averaged trace of 5 independent calculations). In this 20-nm area, the probability of dephosphorylation was set to 0.04. The probability of dephosphorylation in the case of (c) was set 100 times higher than for (b), because we assumed that the same number of CheZ molecules was distributed uniformly in the 2-μm long of the rectangle in (b) and within 20 nm of the rectangle edge in (c).

in a cell stuck on a glass surface. Therefore, we propose that, even in swimming cells, a transient increase and decrease in CheY-P concentration may trigger and regulate the coordinated switching among motors to control the degree of angular change in swimming direction during the tumble. Thus, the chemotaxis system may control the swimming direction of a cell by regulating the degree to which flagellar motors coordinate their switch in rotational direction.

Further questions

To understand the mechanism by which wave-like changes in CheY-P concentration are produced, we performed a simulation of CheY-P molecules diffusing to two motors at different distances from the chemoreceptor patch: motor 1 and 2 were positioned 0.7 μm and 1.2 μm from the patch, respectively (see Fig. 4 legend). We assumed that each motor would switch rotational direction from CCW to CW above some threshold count of CheY-P molecules.

We tested three possibilities. In the first, the rise and fall of CheA kinase activity and the diffusion of CheY-P molecules from the chemoreceptor patch were insufficient to produce wave-like changes in CheY-P concentration. In this case, the motor maintained its CW rotation by the increased CheY-P concentration (Fig. 4a, middle and bottom panels). Next, we simulated the diffusion of CheY-P molecules in the presence of CheZ, which is localized to the cell pole and terminates intracellular signaling by the dephosphorylation of CheY-P in *E. coli*. In our simulation, regardless of the polar localization of CheZ, the increase in CheY-P concentration above the threshold for switching occurred first at motor 1 and then at motor 2 (Fig. 4b and 4c, middle panel). Therefore, the switching from the CCW to the CW direction of motor 1 preceded that of motor 2 (Fig. 4b and 4c, bottom panel). In contrast, only when CheZ was placed at the anterior end of the cell with the receptor patch (Fig. 4c, top panel), the CheY-P concentration fall below the threshold at motor 1 first (Fig. 4b and 4c, middle panels). Thus, the switching delay in both CCW-to-CW and CW-to-CCW that we observed experimentally was qualitatively reproduced only when CheZ was localized to one of the cell poles (Fig. 4b and c, bottom panels).

Lipkow also simulated changes in FliM occupancies (the ratio of FliM subunits binding CheY-P) in motors in different locations on the cell after adding and removing chemotactic signals[45]. She found that FliM occupancy decreased in a motor closer to the chemoreceptor patch prior to decreasing at a more distant motor, only when CheZ was localized to the cellular pole with the receptor patch. These simulations also qualitatively explain our experimental results.

However, to truly understand the intracellular signaling, quantitative measurements are essential: the number of CheY-P molecules generated at the receptor patch and the arrival time and number of CheY-P molecules around each flagellar motor should be clarified experimentally.

Another question arises regarding control of the switching mechanism by CheY-P binding to the motor, since we assume the arrival of the CheY-P signal as the rotational switching of motor. About 34 FliM subunits, and therefore 34 possible CheY-P-binding sites, are present in a motor. Cluzel *et al*. showed a highly cooperativity between CheY-P concentration and the motor's CW bias, which changes drastically from 0 to 1 between CheY-P concentrations of 2–4 μM[34]. On the other hand, Sourjik and Berg estimated FliM occupancy by detecting fluorescence resonance energy transfer (FRET) between FliM and CheY and found that the CheY-P concentration has much less effect on FliM occupancy than on CW bias. From these data, they postulated that the motor switches rotational direction with very little change in FliM occupancy[46].

Some theoretical models have proposed possible mechanisms to explain the highly cooperative switching in response to CheY-P concentration[47–49]. However, the switching mechanism of flagellar motors remains elusive. To reveal the switching mechanism, unknown parameters, such as the number of CheY-P molecules that induces rotational switching in a single flagellar motor, should be quantified. Quantitative detection of FRET between FliM and CheY in a single flagellar motor, rather than a single cell, may help to answer this question.

Summary

High speed and simultaneous imaging of the rotation of two flagellar motors on a single *E. coli* cell has shown that the switching of the rotational direction of multiple motors on a single cell is highly coordinated, with a subsecond delay that clearly correlates with the distance of each motor from the chemoreceptor patch. These findings help to answer a long-standing question about whether the swimming behavior of a cell can be described as a result of the coordinated regulation of rotational direction between flagellar motors. Moreover, we can now infer the process of intracellular signal propagation in a single bacterial cell. These findings offer insight into the mechanism of the bacterial chemotaxis system. Given current progress, we expect to reconstruct the molecular mechanism of bacterial chemotaxis in the near future.

Acknowledgements

We thank Mr. Shun Terasawa, Mr. Hiroto Takahashi, and Mr. Takashi Sagawa (Tohoku University) for conducting critical experiments to clarify the coordinated switching of flagellar motors on an *E. coli* cell.

Work in our laboratory was supported by Grants-in-Aid for Scientific Research from the Ministry of Education, Culture, Sports, Science and Technology and from the Japan Society for the Promotion of Science (to H. F. and A. I.).

References

1. Maeda, T., Wurgler-Murphy, S. M. & Saito, H. A two-component system that regulates an osmosensing MAP kinase cascade in yeast. *Nature* **369**, 242–245 (1994).
2. Schuster, S. C., Noegel, A. A., Oehme, F., Gerisch, G. & Simon, M. I. The hybrid histidine kinase DokA is part of the osmotic response system of Dictyostelium. *EMBO J.* **15**, 3880–3889 (1996).
3. Wilkinson, J. Q., Lanahan, M. B., Yen, H. C., Giovannoni, J. J. & Klee, H. J. An ethylene-inducible component of signal transduction encoded by never-ripe. *Science* **270**, 1807–1809 (1995).
4. Wadhams, G. H. & Armitage, J. P. Making sense of it all: bacterial chemotaxis. *Nat. Rev. Mol. Cell Biol.* **5**, 1024–1037 (2004).
5. Darnton, N. C., Turner, L., Rojevsky, S. & Berg, H. C. On torque and tumbling in swimming *Escherichia coli*. *J. Bacteriol.* **189**, 1756–1764 (2007).
6. Blair, D. F. Flagellar movement driven by proton translocation. *FEBS Lett.* **545**, 86–95 (2003).
7. Manson, M. D., Tedesco, P., Berg, H. C., Harold, F. M. & Van der Drift, C. A protonmotive force drives bacterial flagella. *Proc. Natl. Acad. Sci. USA* **74**, 3060–3064 (1977).
8. Hirota, N., Kitada, M. & Imae, Y. Flagellar motors of alkalophilic *Bacillus* are powered by an electrochemical potential gradient of Na^+. *FEBS Lett.* **132**, 278–280 (1981).
9. Yorimitsu, T. & Homma, M. Na^+-driven flagellar motor of *Vibrio*. *Biochim. Biophys. Acta.* **1505**, 82–93 (2001).
10. Paulick, A., Koerdt, A., Lassak, J., Huntley, S., Wilms, I., Narberhaus, F. & Thormann, K. M. Two different stator systems drive a single polar flagellum in *Shewanella oneidensis* MR-1. *Mol. Microbiol.* **71**, 836–850 (2009).
11. Terahara, N., Krulwich, T. A. & Ito, M. Mutations alter the sodium versus proton use of a *Bacillus clausii* flagellar motor and confer dual ion use on *Bacillus subtilis* motors. *Proc. Natl. Acad. Sci. USA* **105**, 14359–14364 (2008).
12. Ryu, W. S., Berry, R. M. & Berg, H. C. Torque-generating units of the flagellar motor of *Escherichia coli* have a high duty ratio. *Nature* **403**, 444–447 (2000).
13. Inoue, Y., Lo, C. J., Fukuoka, H., Takahashi, H., Sowa, Y., Pilizota, T., Wadhams, G. H., Homma, M., Berry, R. M. & Ishijima, A. Torque-speed relationships of Na^+-driven chimeric flagellar motors in *Escherichia coli*. *J. Mol. Biol.* **376**, 1251–1259 (2008).
14. Nakamura, S., Kami-ike, N., Yokota, J. P., Minamino, T. & Namba, K. Evidence for symmetry in the elementary process of bidirectional torque generation by the bacterial flagellar motor. *Proc. Natl. Acad. Sci. USA* **107**, 17616–17620 (2010).
15. Sowa, Y., Rowe, A. D., Leake, M. C., Yakushi, T., Homma, M., Ishijima, A. & Berry, R. M. Direct observation of steps in rotation of the bacterial flagellar motor. *Nature* **437**, 916–919 (2005).
16. Reid, S. W., Leake, M. C., Chandler, J. H., Lo, C. J., Armitage, J. P. & Berry, R. M. The maximum number of torque-generating units in the flagellar motor of *Escherichia coli* is at least 11. *Proc. Natl. Acad. Sci. USA* **103**, 8066–8071 (2006).
17. Leake, M. C., Chandler, J. H., Wadhams, G. H., Bai, F., Berry, R. M. & Armitage, J. P. Stoichiometry and turnover in single,

functioning membrane protein complexes. *Nature* **443**, 355–358 (2006).
18. Fukuoka, H., Wada, T., Kojima, S., Ishijima, A. & Homma, M. Sodium-dependent dynamic assembly of membrane complexes in sodium-driven flagellar motors. *Mol. Microbiol.* **71**, 825–835 (2009).
19. Delalez, N. J., Wadhams, G. H., Rosser, G., Xue, Q., Brown, M. T., Dobbie, I. M., Berry, R. M., Leake, M. C. & Armitage, J. P. Signal-dependent turnover of the bacterial flagellar switch protein FliM. *Proc. Natl. Acad. Sci. USA* **107**, 11347–11351 (2010).
20. Fukuoka, H., Inoue, Y., Terasawa, S., Takahashi, H. & Ishijima, A. Exchange of rotor components in functioning bacterial flagellar motor. *Biochem. Biophys. Res. Commun.* **394**, 130–135 (2010).
21. Maddock, J. R. & Shapiro, L. Polar location of the chemoreceptor complex in the Escherichia coli cell. *Science* **259**, 1717–1723 (1993).
22. Briegel, A., Ortega, D. R., Tocheva, E. I., Wuichet, K., Li, Z., Chen, S., Müller, A., Iancu, C. V., Murphy, G. E., Dobro, M. J., Zhulin, I. B. & Jensen, G. J. Universal architecture of bacterial chemoreceptor arrays. *Proc. Natl. Acad. Sci. USA* **106**, 17181–17186 (2009).
23. Kim, S. H., Wang, W. & Kim, K. K. Dynamic and clustering model of bacterial chemotaxis receptors: structural basis for signaling and high sensitivity. *Proc. Natl. Acad. Sci. USA* **99**, 11611–11615 (2002).
24. Hazelbauer, G. L., Falke, J. J. & Parkinson, J.S. Bacterial chemoreceptors: high-performance signaling in networked arrays. *Trends. Biochem. Sci.* **33**, 9–19 (2008).
25. Alexander, R. P. & Zhulin, I. B. Evolutionary genomics reveals conserved structural determinants of signaling and adaptation in microbial chemoreceptors. *Proc. Natl. Acad. Sci. USA* **104**, 2885–2890 (2007).
26. Boukhvalova, M., VanBruggen, R. & Stewart, R. C. CheA kinase and chemoreceptor interaction surfaces on CheW. *J. Biol. Chem.* **277**, 23596–23603 (2002).
27. Boukhvalova, M. S., Dahlquist, F. W. & Stewart, R. C. CheW binding interactions with CheA and Tar. Importance for chemotaxis signaling in *Escherichia coli*. *J. Biol. Chem.* **277**, 22251–22259 (2002).
28. Martin, A. C., Wadhams, G. H. & Armitage, J. P. The roles of the multiple CheW and CheA homologues in chemotaxis and in chemoreceptor localization in *Rhodobacter sphaeroides*. *Mol. Microbiol.* **40**, 1261–1272 (2001).
29. Li, M. & Hazelbauer, G. L. Core unit of chemotaxis signaling complexes. *Proc. Natl. Acad. Sci. USA* **108**, 9390–9395 (2011).
30. Sourjik, V. & Berg, H. C. Receptor sensitivity in bacterial chemotaxis. *Proc. Natl. Acad. Sci. USA* **99**, 123–127 (2002).
31. Borkovich, K. A. & Simon, M. I. The dynamics of protein phosphorylation in bacterial chemotaxis. *Cell* **63**, 1339–1348 (1990).
32. Bren, A. & Eisenbach, M. The N terminus of the flagellar switch protein, FliM, is the binding domain for the chemotactic response regulator, CheY. *J. Mol. Biol.* **278**, 507–514 (1998).
33. Sarkar, M. K., Paul, K. & Blair, D. Chemotaxis signaling protein CheY binds to the rotor protein FliN to control the direction of flagellar rotation in *Escherichia coli*. *Proc. Natl. Acad. Sci. USA* **107**, 9370–9375 (2010).
34. Cluzel, P., Surette, M. & Leibler, S. An ultrasensitive bacterial motor revealed by monitoring signaling proteins in single cells. *Science* **287**, 1652–1655 (2000).
35. Scharf, B. E., Fahrner, K. A., Turner, L. & Berg, H. C. Control of direction of flagellar rotation in bacterial chemotaxis. *Proc. Natl. Acad. Sci. USA* **95**, 201–206 (1998).
36. Cantwell, B. J., Draheim, R. R., Weart, R. B., Nguyen, C., Stewart, R. C. & Manson, M. D. CheZ phosphatase localizes to chemoreceptor patches via CheA-short. *J. Bacteriol.* **185**, 2354–2361 (2003).
37. Jones, C. J. & Aizawa, S. The bacterial flagellum and flagellar motor: structure, assembly and function. *Adv. Microb. Physiol.* **32**, 109–172 (1991).
38. Macnab, R. M. & Han, D. P. Asynchronous switching of flagellar motors on a single bacterial cell. *Cell* **32**, 109–117 (1983).
39. Ishihara, A., Segall, J. E., Block, S. M. & Berg, H. C. Coordination of flagella on filamentous cells of *Escherichia coli*. *J. Bacteriol.* **155**, 228–237 (1983).
40. Terasawa, S., Fukuoka, H., Inoue, Y., Sagawa, T., Takahashi, H. & Ishijima, A. Coordinated reversal of flagellar motors on a single *Escherichia coli* cell. *Biophys. J.* **100**, 2193–2200 (2011).
41. Fukuoka, H., Sowa, Y., Kojima, S., Ishijima, A. & Homma, M. Visualization of functional rotor proteins of the bacterial flagellar motor in the cell membrane. *J. Mol. Biol.* **367**, 692–701 (2007).
42. Bourret, R. B., Hess, J. F. & Simon, M. I. Conserved aspartate residues and phosphorylation in signal transduction by the chemotaxis protein CheY. *Proc. Natl. Acad. Sci. USA* **87**, 41–45 (1990).
43. Turner, L., Ryu, W. S. & Berg, H. C. Real-time imaging of fluorescent flagellar filaments. *J. Bacteriol.* **182**, 2793–2801 (2000).
44. Vladimirov, N., Lebiedz, D. & Sourjik, V. Predicted auxiliary navigation mechanism of peritrichously flagellated chemotactic bacteria. *PLoS. Comput. Biol.* **6**, e1000717 (2009).
45. Lipkow, K. Changing cellular location of CheZ predicted by molecular simulations. *PLoS Comput. Biol.* **2**, e39 (2006).
46. Sourjik, V. & Berg, H. C. Binding of the *Escherichia coli* response regulator CheY to its target measured in vivo by fluorescence resonance energy transfer. *Proc. Natl. Acad. Sci. USA* **99**, 12669–12674 (2002).
47. Duke, T. A., Le Novere, N. & Bray, D. Conformational spread in a ring of proteins: a stochastic approach to allostery. *J. Mol. Biol.* **308**, 541–553 (2001).
48. Bai, F., Branch, R. W., Nicolau, D. V. Jr., Pilizota, T., Steel, B. C., Maini, P. K. & Berry, R. M. Conformational spread as a mechanism for cooperativity in the bacterial flagellar switch. *Science* **327**, 685–689 (2010).
49. Korobkova, E., Emonet, T., Vilar, J. M., Shimizu, T. S. & Cluzel, P. From molecular noise to behavioural variability in a single bacterium. *Nature* **428**, 574–578 (2004).